Published in final edited form as:
Bioconjug Chem. 2006 ; 17(4): 920–927.

Self-Assembled Quantum Dot-Peptide Bioconjugates for Selective Intracellular Delivery

James B. Delehanty[†,*], **Igor L. Medintz**[†], **Thomas Pons**[‡,€], **Philip E. Dawson**[§], **Florence M. Brunel**[§], and **Hedi Mattoussi**[‡,*]

†*Center for Bio/Molecular Science and Engineering, Code 6900, U.S. Naval Research Laboratory, Washington, DC 20375*

‡*Optical Sciences Division, Code 5611, U.S. Naval Research Laboratory, Washington, DC 20375*

§*Departments of Cell Biology & Chemistry and the Skaggs Institute for Chemical Biology, The Scripps Research Institute, La Jolla, CA 92037*

€*Chemical & Biomolecular Engineering Department, Johns Hopkins University, Baltimore, MD 21218*

Abstract

We demonstrate the use of self-assembled luminescent semiconductor quantum dot (QD) - peptide bioconjugates for the selective intracellular labeling of several eukaryotic cell lines. A bifunctional oligoarginine cell penetrating peptide (based on the HIV-1 Tat protein motif) bearing a terminal polyhistidine tract was synthesized and used to facilitate the transmembrane delivery of the QD bioconjugates. The polyhistidine sequence allows the peptide to self-assemble onto the QD surface via metal-affinity interactions while the oligoarginine sequence allows specific QD delivery across the cellular membrane and intracellular labeling as compared to non-conjugated QDs. This peptide-driven delivery is concentration-dependent and thus can be titrated. Upon internalization, QDs display a punctate-like staining pattern in which some, but not all, of the QD signal is co-localized within endosomes. The effects of constant versus limited exposure to QD-peptide conjugates on cellular viability are evaluated by a metabolic specific assay and clear differences in cytotoxicity are observed. The efficacy of using peptides for selective intracellular delivery is highlighted by performing a multicolor QD labeling, where we found that the presence or absence of peptide on the QD surface controls cellular uptake.

Keywords

Quantum Dot; Fluorophore; Peptide; HIV-1 Tat; Cellular Labeling; Transmembrane; Endocytosis; Translocation

Introduction

Luminescent semiconductor nanocrystals or quantum dots (QDs)[1] are a relatively new class of fluorescent probe whose unique optical properties suggest that they are superior to conventional organic dyes for many biological applications (1-5). QD properties include high quantum yield, broad absorption spectra, large achievable Stokes shifts, narrow symmetric,

*To whom correspondence should be addressed: Email: jdelehanty@cbmse.nrl.navy.mil. Phone: 202-767-0291. Fax: 202-767-9594; hedimat@ccs.nrl.navy.mil. Phone 202-767-9473. Fax: 202-404-8114.

[1]Abbreviations used: AF546-transferrin, AlexaFluor 546-conjugtaed transferring; CPP, cell penetrating peptide; DHLA, dihydrolipoic acid; QD, quantum dot; PBS, phosphate buffered saline; PL, photoluminescence.

size-tunable emission spectra and exceptional resistance to photo- and chemical degradation (2-6). These properties are particularly appealing for the visualization of cellular processes as they can potentially facilitate long-term and multi-color labeling of both fixed and living cells. An intensive exploration is currently underway by several groups to optimize methods for the intracellular delivery of QDs and QD bioconjugates and to characterize their long-term *in vivo* photophysical properties.

Three important criteria must be met for the successful development of QDs and QD bioconjugates as reliable reagents for cellular labeling and *in vivo* imaging. First, hydrophilic QD probes must be prepared in a facile and controlled manner. Second, their intracellular uptake must exhibit an element of selective delivery and the QD probes must be able to access various subcellular compartments. Third, the QD bioconjugates must elicit minimal or no cytotoxicity over the time course required for efficient cellular delivery, labeling, subsequent targeting and sensing. Reports describing QD bioconjugates that meet all three of these criteria, however, remain limited.

A few strategies for developing QD-cell penetrating peptide (CPP) bioconjugates for cellular delivery have been attempted and mixed results have been demonstrated in terms of providing effective cellular transmembrane delivery and labeling. Silver and Ou used commercially available QDs functionalized with streptavidin/polyethylene glycol and complexed to both biotinylated and non-biotinylated peptides expressing a 9-mer poly-arginine sequence (7). These bioconjugates were delivered to lysosomes and formed aggregates in both HeLa and baby hamster kidney cells. Coating the same QDs with protein A and complexing them with poly-L-lysine also produced equally effective cellular delivery, suggesting that charge alone may be the dominant translocation mediator in these cells. Lagerholm attached 25- to 50-fold excess of a biotinylated 9-mer poly-arginine containing peptide to streptavidin QDs and found intracellular labeling in Swiss 3T3, HeLa and MG63 cells with a brightness two orders of magnitude stronger than unconjugated QDs alone (8). Rozenzhak used a noncovalently complexed 21-residue peptide carrier for cellular delivery of QDs into HeLa cells (9). This peptide, which is believed to function independently of endocytosis, consists of a hydrophobic tryptophan-rich domain for efficient membrane translocation and a lysine-rich domain for solubility. Efficient intracellular delivery of QDs with punctate cytoplasmic staining was reported using this peptide carrier. Hoshino reported that 48-62 copies of an 11-mer poly-arginine containing sequence covalently attached to QDs facilitated their rapid cellular uptake and localization to the nucleus in Vero cells (10). In contrast, Derfus reported that complexing QDs with a Chariot peptide actually decreased HeLa cell uptake to levels below those of uncomplexed QDs (11). A similar TAT protein-derived sequence has been shown to efficiently mediate the nuclear translocation of gold nanoparticles that were less than 5nm in diameter (12).

Strategies for the intracellular delivery of QDs have relied largely on the use of receptor-mediated or non-specific endocytosis (1,13). In a detailed report, Jaiswal et al. demonstrated passive endocytotic uptake of hydrophilic QDs capped with dihydrolipoic acid (DHLA) by incubating HeLa cells with solutions containing QDs at concentrations of 400 – 600 nM QDs for 3-4 hours (1). QDs entering cells by this pathway remained largely sequestered within endocytic vesicles for several hours (1,11). Other methods for the cellular uptake of QDs that have been reported include: electroporation (14), cationic transfection reagents (11,15) and microinjection (11). Each of these methods has certain drawbacks, however. For example, microinjection is a limited throughput process, as individual cells must be manipulated one at a time, while electroporation necessitates forming pores in the cellular membrane. Peptide-mediated delivery on the other hand remains one of the more attractive methods due to the ease of use. This involves complexing QDs with cell penetrating peptides (CPP) to facilitate their transmembrane delivery. These peptide motifs are most often based on the HIV-1 Tat peptide

(16), antennapedia (17), and transportan sequences (18). The classical or core CPP motif is derived from the HIV-1 Tat peptide and usually consists of 7-11 consecutive repeats of positively charged arginine residues (19). While the mechanism of CPP-mediated membrane translocation remains under investigation, increasing evidence points to the involvement of several types of endocytosis (20-25).

In this report, we describe the development and characterization of self-assembled QD-peptide bioconjugates for the specific intracellular delivery into several eukaryotic cell lines. A polyhistidine appended peptide expressing an 8-mer poly-arginine sequence is first self-assembled onto DHLA-capped CdSe-ZnS QDs, then used to facilitate QD transmembrane delivery. We found that once internalized some, but not all, of the QD staining colocalizes with endosomal compartments. We also found that peptide-mediated QD uptake is dependent on conjugate concentration while exposure of cells to non-conjugated QDs results in negligible intracellular labeling. Significant differences in cellular toxicity are also noted for chronic (long-term) versus acute (short-term) cell incubation with QD-peptide conjugates. Selective intracellular labeling is further highlighted by performing a multicolor QD labeling experiment, where the presence or absence of peptide on the QD surface was found to determine whether cellular uptake can occur or not.

Materials and Methods

Quantum Dots

CdSe-ZnS core-shell QDs with emission maxima centered at 510 nm and 551 nm were synthesized and made hydrophilic by exchanging the native trioctylphosphine/ trioctylphosphine oxide (TOP/TOPO) capping shell with DHLA ligands as described previously (26). The QDs are identified by their wavelength of maximum emission, e.g., a sample of 510 nm QDs designates a population of QDs which exhibits maximum photoluminescence centered at 510 nm (see Figure 1B).

Peptide Synthesis

The cell-penetrating peptide (CPP) used in this study is comprised of the sequence $(His)_8$ -Trp-Gly-Leu-Ala-Aib-Ser-Gly-$(Arg)_8$-amide, where Aib is α-amino isobutyric acid and the C-terminus is blocked with an amide. The N-terminal polyhistidine $(His)_8$ tract mediates self-assembly onto DHLA-capped CdSe-ZnS QDs (27-34). The peptide was synthesized manually using *in-situ* neutralization cycles for Boc-solid phase peptide synthesis on 0.2 mmol MBHA resin (4-Methylbenzhydryl-amine, Peptides International, Louisville, KY) using 1.1 mmol amino acid, 1.0 mmol HCTU([2-(1*H*-6-chlorobenzotriazol-1-yl)-1,1,3,3-tetramethyluronium-hexafluoro-phosphate]), 2 mL of 0.5 M solution in DMF) and 0.5 mL DIEA (N,N-(Diisopropyl)aminomethylpolystyrene) (35). Coupling times were typically 20 min. Following chain assembly, the peptide was cleaved from the resin with hydrofluoric acid and 10% anisole for 1h at 0°C, purified by HPLC, and characterized by electrospray ionization mass spectrometry using an API-III triple quadruple mass spectrometer (Sciex, Thornhill, CA). The peptide mass was calculated from the experimental mass to charge (m/z) ratios from all of the observed protonation states of a peptide using MacSpec software (Sciex). The observed peptide mass agreed with the calculated average mass within 0.5 Da.

Cell Culture

HEK 293T/17 and COS-1 cell lines (both from ATCC, Manassas, VA) were cultured as exponentially growing subconfluent monolayers in complete growth medium (Dulbecco's Modified Eagle's Medium (DMEM) supplemented with 4 mM L-glutamine, 1 mM sodium pyruvate, 1% (v/v) antibiotic/antimycotic and 10% (v/v) heat inactivated fetal bovine serum

(FBS)). Cells were grown on 60-mm dishes and incubated at 37°C under 5% CO_2 atmosphere. A subculture was performed every 3-4 days.

Assembly of Quantum Dot-Cell Penetrating Peptide Bioconjugates

Self-assembled QD-CPP bioconjugates were prepared by incubating stock solutions of 1 μM QD with appropriate ratios of desalted CPP in 10 mM sodium tetraborate buffer pH 9.6 for at least one hour. QD-CPP assemblies were diluted into complete growth medium immediately prior to use. Once diluted into growth medium, QD-CPP assemblies typically remained in solution for >24 hours. We have found that if the peptide was not desalted prior to use, there were instances where the QD-CPP conjugates precipitated.

Cellular Uptake of Quantum Dot-Peptide Assemblies

All cellular internalization experiments were performed on microscope slides fitted with multiwell forms as described previously (36). Aminopropylsilane functionalized glass slides (GAPSII, Corning) were coated overnight with 50 μg/mL fibronectin (Sigma) in sodium bicarbonate buffer (pH 8.5). Slides were washed twice with distilled water, dried under a stream of nitrogen, and an 8-well adhesive silicone form (Schleicher and Schuell) was affixed. Cells (2×10^4 cells/well) were seeded into the wells and cultured overnight. For delivery experiments, QDs or QD-CPP assemblies were diluted into complete culture medium and incubated with the cells at 37°C for one hour. For experiments aimed at assessing QD-CPP co-localization with endosomes, an Alexa Fluor 546-transferrin conjugate (AF546-transferrin, Molecular Probes) was included with the assemblies at a final concentration of 40 μg/mL. After incubation, excess unbound QDs were removed by washing three times with phosphate buffered saline (PBS, pH 7.4). Cells were then fixed in 3.7% paraformaldehyde for 10 minutes at room temperature. The cells were washed twice with PBS and mounted in ProLong Antifade mounting media containing DAPI (Molecular Probes).

Fluorescence Microscopy and Image Analysis

Intracellular distribution of QD staining was analyzed by bright field and epifluorescence microscopy using a Nikon ES800 upright fluorescence microscope equipped with a 40× lens. Images were collected using standard Nikon filter sets for DAPI, FITC (for 510 QDs), and TRITC (for AF546-transferrin). Merged images were generated using Adobe PhotoShop. Images of cell cultures incubated a mixture of two-color QDs were collected by scanning confocal fluorescence microscopy using a Zeiss LSM 510 inverted microscope equipped with a 60× oil immersion lens. Images were collected using the following excitation (ex) lines and emission (em) filters: 510 QDs, 488 nm (ex), 490-510 nm (em); 551 QDs, 488 nm (ex), 545-585 nm (em); AF546-transferrin, 546 nm (ex), 570 nm longpass filter (em). Phase contrast images were collected using 633 nm laser illumination. Composite merged images were produced using the LSM Image Browser (Zeiss).

Cytotoxicity Assays

Cellular toxicity of the CPP, unconjugated QDs and QD-CPP assemblies were assessed using the CellTiter 96 Cell Proliferation Assay (Promega, Madison WI) according to the manufacture's instructions. This assay is based upon the conversion of a tetrazolium substrate to a formazan product by viable cells at the assay end point (37). The formazan product absorbs at 570 nm. Cells (1×10^4 cells/well) were cultured in 96-well microtiter plates in complete growth medium in the presence of increasing concentrations of QDs, CPP or QD-CPP assemblies. For the assessment of chronic toxicity, the QD materials were applied to cells and incubated for 24 hours prior to assaying the number of viable cells. For acute toxicity studies, the materials were incubated with the cells for one hour, removed, and the media was replaced

with complete growth media. Cells were then cultured for 24 hours prior to assaying for cell viability.

Results and Discussion

Formation of Quantum Dot-CPP Assemblies

QD-peptide bioconjugates were formed by mixing the $(His)_8$-terminated CPP with DHLA-capped QDs for at least 30 minutes prior to use (Figure 1A). This allows the CPP to self-assemble onto the QD surface. We have previously shown that proteins and peptides expressing terminal polyhistidine sequences self-assemble onto DHLA-capped CdSe-ZnS QDs via metal-affinity coordination (27-34). Furthermore, this conjugation scheme allows control over the peptide-to-QD ratio in these conjugates. The dissociation constant of this interaction is estimated to be stronger than most antibody-antigen interactions ($K_d \geq 10^{-9}$ M) (38). We have found that upon addition of CPP to QD solutions a substantial increase in the solution photoluminescence (PL) intensity is measured; at a ratio of ~10 peptides per QD-conjugate ~100% enhancement in solution PL is measured in comparison to a control solution of unconjugated QDs. This observation is consistent with our previous results on self-assembled QD-protein-His and QD-peptide-His conjugates and we used it as an indicator of QD-CPP bioconjugate formation (26, 31, 39).

Cellular Uptake of Quantum Dot-CPP Assemblies

To determine the efficiency of CPP-mediated internalization, cells were incubated with either non-conjugated QDs or QD-CPPs assembled at QD:CPP ratios of 1:5, 1:25, or 1:50. Figure 2 shows epifluorescence/phase contrast image overlays of HEK 293T/17 cells that were incubated with non-conjugated 510 nm-emitting QDs or with a concentration series of QD-CPP assemblies (ratio of 1:50). The images clearly show that the presence of CPPs on the QD surface resulted in the concentration-dependent cellular uptake of the assemblies, with the highest intracellular QD fluorescence observed for cells incubated with solutions containing higher concentrations of QDs (Figure 2A). Punctate QD fluorescence was dispersed throughout the cytoplasm as well as in close proximity to the cell nuclei (perinuclear), but no nuclear staining was apparent. When the cells were incubated with lower concentrations of QD-CPP assemblies, the degree of cellular uptake was noticeably reduced (Figure 2 B, C). In the absence of CPP, no intracellular QD fluorescence was observed (Figure 2D). Similarly, control experiments performed with a non-$(His)_8$-CPP peptide resulted in no noticeable cellular uptake. We also observed essentially no difference in the efficiency of uptake between QD-CPPs assembled at ratios of 1:50 and 1:25. However, a noticeable decrease in uptake occurred when the ratio was decreased to 1:5 (data not shown). Further, we observed no detectable fluorescence signal remaining on the plasma membrane, indicating a negligible degree of nonspecific binding of the QD-CPP assemblies to the cell surface after washing. These results provide strong evidence that complexing the CPPs with QDs allows for specific cellular internalization relative to the same concentration of non-conjugated QDs and also demonstrate the concentration dependent nature of the peptide-facilitated uptake. We should emphasize that similar experiments performed with COS-1 cells resulted in an approximately 2- to 3-fold lower efficiency of QD-CPP conjugate uptake and likely point to differences between the two cell lines used. Nonetheless, the amount of delivered QD cargos was large enough to produce a strong fluorescence signal and to carry out additional comparative experiments.

To monitor the fate of the internalized QD-CPP assemblies in HEK293T/17 and COS-1 cells, we examined the intracellular distribution of QD-CPP assemblies that were simultaneously delivered with AlexaFluor 546-conjugated transferrin (AF546-transferrin). Transferrin is an 80 kDa serum glycoprotein that mediates iron uptake in vertebrate cells via receptor-mediated endocytosis and labeled transferrin is commonly used to monitor the endocytic pathway (40,

41). To visualize the nuclei, the cells were also stained with DAPI (Figure 3, A and E). In both cell lines, a punctate and vesicular QD fluorescence pattern was observed within the cytoplasm and within perinuclear spaces (Figure 3, B and F). This punctate appearance is not unexpected for this type of DHLA-capped QD when present within the slightly acidic cellular environment and is consistent with previously published results (1,11). When the QD fluorescence pattern was merged with the vesicular staining pattern of AF546-transferrin (Figure 3, C and G), it was evident that at least a portion of the internalized QD-CPP assemblies were co-localized within endosomes (Figure 3, D and H). Simultaneous incubation with AF546-transferrin did not alter QD-CPP uptake or staining in any manner. Further, when cells were incubated with the QD-CPP assemblies at 4° C, where endocytosis is inhibited, cellular uptake was completely eliminated (data not shown). These results strongly suggest a role for endocytosis in the uptake of the QD-CPP assemblies. Recent studies using live-cell imaging and FACS analysis have also established that arginine-rich CPPs and their conjugated cargos are internalized by endocytosis (24,25,42).

Selective Quantum Dot-CPP Cellular Uptake

To investigate the ability of cells to discriminate between two QD populations (colors) presenting distinct surface functionalities, HEK 293T/17 cells were incubated for one hour with a mixture of 510 nm QD-CPP conjugates and unconjugated 551 nm QDs. The cells were then fixed and examined by scanning confocal fluorescence microscopy. As shown in Figure 4A, when cells were incubated with 510 nm QD-CPP assemblies (at a concentration of 250 nM QD) and unconjugated 551 nm QDs (at a concentration of 60 nM QD), internalization of only the 510 nm QDs was observed[2]. No intracellular QD fluorescence corresponding to the 551 nm QDs was observed (Figure 4B). Consistent with our previous experiments, the pattern of intracellular QD fluorescence was punctate in nature and was excluded from the nucleus. However, in contrast to our previous observations using epifluorescence microscopy, the more sensitive confocal analysis used here indicated a higher degree of intracellular QD fluorescence than what was previously measured above (see Figure 3) as evidenced by the QD signal dispersed nearly homogeneously throughout the cytoplasm. When the pattern of QD fluorescence was compared to that of AF546-transferrin (Figure 4C), a modest degree of overlap was observed indicating partial co-localization of QDs within endosomes (Figure 4D). The majority of the QDs appeared to be excluded from endocytotic vesicles (Figure 4E). The presence of the QDs within the cytoplasm coupled with the lack of QD signal within the nucleus is notable in light of previous investigations which have shown that paraformaldehyde or methanol fixation protocols can cause an artificial redistribution of CPPs and CPP-conjugates from the cytoplasm to the nucleus (42). The fact that we observed no nuclear translocation suggests that the radius of the QD (hydrodynamic radius ~5-6 nm) precluded the passive diffusion of the QD-CPP assembly through the nuclear pore complex whose hydrodynamic radius is approximately 5 nm (43).

In the converse experiment, HEK 293T/17 cells were incubated with mixtures of 551 nm QD-CPP assemblies (at a concentration of 250 nM QDs) and unconjugated 510 nm QDs (at a concentration of 60 nM QDs). Again, the cells internalized only QDs that were complexed with CPPs as only signal corresponding to the 551 nm QDs was apparent (Figure 4G). We did, however, note that the overall intracellular fluorescence of the internalized 551 nm QDs was lower than that previously observed for the CPP-mediated delivery of 510 nm QDs. This difference is attributable to the differential excitation efficiency of the two QD species with the 488 nm laser line, which corresponds to the first absorption peak of the 510 nm QDs while it coincides with the absorption “valley” of the 551 nm QDs (see Figure 1B). Also in contrast

[2]For the unconjugated QDs, a concentration of 60 nM QDs was used since our previous results demonstrated that no uptake of unconjugated QDs occurred when they were present at a concentration of 250 nM (see Figure 2).

with the internalization of 510 nm QD-CPP assemblies, we found that the 551 nm QDs were almost exclusively co-localized with the transferrin conjugate, indicating the sequestration of the 551 QDs within endosomes (Figure 4, H and I). Minimal 551 nm QD fluorescence was dispersed within the cytoplasm (Figure 4J). While it is likely that the differential excitation efficiencies of the two QD species also contributes to these observed differences, it is worth noting that previous studies have demonstrated the ability of poly-$_L$-histidine to increase the endosomal escape of plasmid DNA via the membrane destabilization of acidic endocytotic vesicles following protonation of the imidazole groups (44-46). It is possible that the CPP plays a contributing role in aiding the endosomal escape of the QD-CPP assemblies as the CPP peptide contains a $(His)_8$ sequence.

Confocal analysis of these same samples also confirmed that the QD fluorescence was localized exclusively to the cell interior with no evidence of nonspecifically bound QDs on the cell membrane. Figure 5 (panels A – E) shows a sequential z-step analysis taken through HEK 293T/17 cells incubated with a mixture of 510 nm QD-CPP conjugates and unconjugated 551 nm QDs. Standard washing of the cells with PBS was sufficient to remove all loosely bound QDs from the cell surface. This is in contrast to other reports wherein trypsin digestion (42) or modification of the QD surface (e.g., with poly(ethylene glycol) ligands) (47) were required to remove nonspecific QD binding to the cell surface.

Cytotoxicity of Quantum Dot-CPP Assemblies

The cytotoxicity of the free CPP, unconjugated QDs, and QD-CPP assemblies was assessed by monitoring their ability to inhibit cellular proliferation. Using a colorimetric tetrazolium-based cell proliferation assay, we assessed the toxicity of both short-term (acute) and long-term (chronic) incubation of COS-1 cells and HEK 293T/17 cells to these materials. Under conditions of acute exposure, wherein cells were incubated with the materials for one hour followed by rinsing and subsequent culture for 24 hours, we observed no significant change in proliferation for the CPP (12.5 μM highest concentration tested), unconjugated QDs (250 nM QD highest concentration tested), or QD-CPP assemblies (CPP:QD ratio of 50:1, 12.5 μM CPP: 250 nM QD highest concentration tested) in either COS-1 or HEK 293T/17 cell lines relative to the untreated control (Figure 6 A, B respectively). These exposure conditions are identical to those used to achieve the intracellular delivery of QD-CPP assemblies described in this report and illustrate that the acute exposure of either cell line to the QD-CPP assemblies does not result in any appreciable change in cell viability at the concentrations required for efficient cellular uptake. Under conditions of chronic exposure (incubation for 24 hours or longer), however, a distinct dose-dependent cytotoxic effect of the materials was observed (Figure 6 C, D respectively). For both cell lines, the QD-CPP assemblies had the greatest effect on cell proliferation, eliciting a slightly higher degree of toxicity in HEK 293T/17 cells than in COS-1 cells. This result is consistent with our observations of the slightly higher efficiency of QD-CPP internalization by HEK 293T/17 cells. The unconjugated QDs were slightly less toxic than the QD-CPP assemblies. While the free CPP had only a slight effect on the proliferation of COS-1 cells, it was increasingly toxic to HEK 293T/17 cells at concentrations greater than ~750 nM.

While other studies have characterized the toxicity of unconjugated QDs (48,49) and QD bioconjugates (1) or free CPPs (50) and their associated cargos (51), reports detailing the comparative effects of acute versus chronic incubation conditions across multiple cell lines remain limited. Importantly, our results demonstrate not only distinct differences between the two incubation conditions but may also point to cell type-dependent differences in the degree of toxicity.

Conclusions

We have demonstrated the effective use of cell penetrating peptides to drive the non-invasive intracellular delivery of hydrophilic QD cargos. The approach was applied to two different eukaryotic cell lines, HEK 293T/17 and COS-1. The QD-peptide bioconjugates described in this report are prepared by the facile self-assembly of a polyhistidine-appended cell penetrating peptide with DHLA-capped CdSe-ZnS core shell QDs. This assembly process may ultimately allow for the generation of mixed peptide surfaces, wherein each different peptide imparts a unique functionality to the resulting bioconjugate. A similar strategy has been suggested by Weiss (52).

We found that the level of intracellular uptake of the QD-CPP assemblies depends on the QD concentration, the number of QD-associated CPPs, and the cell type used. In the absence of CPP, the extent of QD internalization is essentially non-existent. Our results show that QD fluorescence is localized to the cell interior with no nonspecific binding of QD-CPP to the cell surface. While other studies have detailed the use of covalent modification of the QD surface with poly(ethylene glycol) (47) ligands or trypsin digestion of cells (42) to reduce the nonspecific binding of QDs, we found that the QD-CPP assemblies were easily removed from the cell surface by washing with PBS. Consistent with other reports that have established the role of endocytosis in the uptake of arginine-rich CPPs and their cargos (24,25,42), the partial co-localization of the internalized QD-CPPs within endosomes and the complete elimination of their uptake upon incubation at 4 °C provide strong evidence for the role of endocytosis in the uptake of our QD-CPP assemblies. Further, the use of QD-CPP conjugates allows for the intracellular delivery of QDs at lower concentrations and with shorter incubation times compared to other reports which have used nonspecific endocytosis of unconjugated QDs (1).

We also observed significant differences between acute and chronic exposure of cells to the QD-CPP complexes. While our chronic exposure results are consistent with those previously reported for unconjugated QDs (49), CPPs (51), and QD bioconjugates (7), the acute toxicity data presented here represents the first description of the minimal cytotoxicity associated with a delivery time course required for successful intracellular uptake. These results are very promising and indicate that cells can be exposed to these assemblies, effectively labeled, and used without significant alteration of their viability or function.

The fine degree of controlled QD-CPP delivery coupled with the minimal toxicity associated with that delivery now sets the stage for more elegant *in vitro* and *in vivo* labeling applications, such as the simultaneous delivery and tracking of multiple color QDs to different intracellular compartments (molecular “bar-coding”). The use of multi-peptide labeled QDs will likely facilitate these studies where each peptide contributes a different function such as cellular uptake, endosomal escape and organelle targeting.

Acknowledgements

The authors acknowledge NRL and L. Chrisey at the Office of Naval Research (ONR grant # N001404WX20270). T. Pons acknowledges support from the Foundation pour la Recherche Midicale. We are also grateful to Michelle Husain and the Integrated Imaging Center at Johns Hopkins University for their assistance with the confocal microscopy.

References

1. Jaiswal JK, Mattoussi H, Mauro JM, Simon SM. Long-term multiple color imaging of live cells using quantum dot bioconjugates. Nat Biotechnol 2003;21:47–51. [PubMed: 12459736]
2. Alivisatos AP, Gu W, Larabell CA. Quantum dots as cellular probes. Ann Rev Biomed Eng 2005;7:55–76. [PubMed: 16004566]

3. Alivisatos P. The use of nanocrystals in biological detection. Nat Biotechnol 2004;22:47–52. [PubMed: 14704706]
4. Medintz IL, Uyeda H, Goldman ER, Mattoussi H. Quantum dot bioconjugates for imaging, labeling and sensing. Nat Mater 2005;4:435–446. [PubMed: 15928695]
5. Parak WJ, Gerion D, Pellegrino T, Zanchet D, Micheel C, Williams SC, Boudreau R, Le Gros MA, Larabell CA, Alivisatos AP. Biological applications of colloidal nanocrystals. Nanotechnology 2003;14:R15–R27.
6. Parak W, Pellegrino T, Plank C. Labelling of cells with quantum dots. Nanotechnology 2005;16:R9–R25.
7. Silver J, Ou W. Photoactivation of quantum dot fluorescence following endocytosis. Nano Letters 2005;5:1445–1449. [PubMed: 16178255]
8. Lagerholm BC, Weinreb GE, Thompson NL, Jacobson K. Multicolor coding of quantum dots with cationic peptide coated quantum dots. Nano Letters 2004;4:2019–2022.
9. Rozenzhak SM, Kadakia MP, Caserta TM, Westbrook TR, Stone MO, Naik RR. Cellular internalization and targeting of semiconductor quantum dots. Chem Commun 2005;17:2217–2219.
10. Hoshino A, Fujioka K, Oku T, Nakamura S, Suga M, Yamaguchi Y, Suzuki K, Yasuhara M, Yamamoto K. Quantum dots targeted to the assigned organelle in living cells. Microbiol and Immunol 2004;48:985–994. [PubMed: 15611617]
11. Derfus AM, Chan WCW, Bhatia SN. Intracellular delivery of quantum dots for live cell labeling and organelle tracking. Adv Mater 2004;16:961–966.
12. de la Fuente JM, Berry Catherine C. Tat peptide as an efficient molecule to translocate gold nanoparticles into the cell nucleus. Bioconjugate Chem 2006;16:1176–1180.
13. Chan WC, Nie S. Quantum dot bioconjugates for ultrasensitive nonisotopic detection. Science 1998;281:2016–2018. [PubMed: 9748158]
14. Chen FQ, Gerion D. Fluorescent CdSe/ZnS nanocrystal-peptide conjugates for long-term, nontoxic imaging and nuclear targeting in living cells. Nano Letters 2004;4:1827–1832.
15. Voura EB, Jaiswal JK, Mattoussi H, Simon SM. Tracking early metastatic progression with quantum dots nanocrystals and emission scanning microscopy. Nat Med 2004;10:993–998. [PubMed: 15334072]
16. Futaki S. Membrane-permeable arginine-rich peptides and the translocation mechanisms. Adv Drug Deliver Rev 2005;57:547–548.
17. Derossi D, Joliot AH, Chassaing G, Prochiantz A. The third helix of the Antennapedia homeodomain translocates through biological membranes. J Biol Chem 1994;269:10444–10450. [PubMed: 8144628]
18. Pooga M, Hallbrink M, Zorko M, Langel U. Cell penetration by transportan. Faseb J 1998;12:67–77. [PubMed: 9438412]
19. Zhao M, Weissleder R. Intracellular cargo delivery using tat peptide and derivatives. Med Res Rev 2004;24:1–12. [PubMed: 14595670]
20. Richard JP, Melikov K, Brooks H, Prevot P, Lebleu B, Chernomordik LV. Cellular uptake of unconjugated TAT peptide involves clathrin-dependent endocytosis and heparan sulfate receptors. J Biol Chem 2005;280:15300–15306. [PubMed: 15687490]
21. Drin G, Cottin S, Blanc E, Rees AR, Temsamani J. Studies on the internalization mechanism of cationic cell-penetrating peptides. J Biol Chem 2003;278:31192–311201. [PubMed: 12783857]
22. Fittipaldi A, Ferrari A, Zoppe M, Arcangeli C, Pellegrini V, Beltram F, Giacca M. Cell membrane lipid rafts mediate caveolar endocytosis of HIV-1 Tat fusion proteins. J Biol Chem 2003;278:34141–34149. [PubMed: 12773529]
23. Saalik P, Elmquist A, Hansen M, Padari K, Saar K, Viht K, Langel U, Pooga M. Protein cargo delivery properties of cell-penetrating peptides. A comparative study. Bioconjugate Chem 2004;15:1246–1253.
24. Wadia JS, Stan RV, Dowdy SF. Transducible TAT-HA fusogenic peptide enhances escape of TAT-fusion proteins after lipid raft macropinocytosis. Nat Med 2004;10:310–5. [PubMed: 14770178]
25. Kaplan IM, Wadia JS, Dowdy SF. Cationic TAT peptide transduction domain enters cells by macropinocytosis. J Control Release 2005;102:247–53. [PubMed: 15653149]

26. Mattoussi H, Mauro JM, Goldman ER, Anderson GP, Sundar VC, Mikulec FV, Bawendi MG. Self-Assembly of CdSe-ZnS Quantum Dot Bioconjugates Using an Engineered Recombinant Protein. J Am Chem Soc 2000;122:12142–12150.
27. Goldman E, Medintz IL, Whitley J, Hayhurst A, Clapp A, Uyeda H, Deschamps J, Lassman M, Mattoussi H. A hybrid quantum dot-antibody fragment fluorescence resonance energy transfer-based TNT sensor. J Am Chem Soc 2005;127:6744–6751. [PubMed: 15869297]
28. Clapp AR, Medintz IL, Fisher BR, Anderson GP, Mattoussi H. Can luminescent quantum dots be efficient energy acceptors with organic dye donors? J Am Chem Soc 2005;127:1242–1250. [PubMed: 15669863]
29. Clapp AR, Medintz IL, Mauro JM, Fisher BR, Bawendi MG, Mattoussi H. Fluorescence Resonance Energy Transfer Between Quantum Dot Donors and Dye-Labeled Protein Acceptors. J Am Chem Soc 2004;126:301–310. [PubMed: 14709096]
30. Medintz IL, Konnert JH, Clapp AR, Stanish I, Twigg ME, Mattoussi H, Mauro J Matthew, Deschamps JR. A fluorescence resonance energy transfer derived structure of a quantum dot-protein bioconjugate nanoassembly. Proc Natl Acad Sci USA 2004;101:9612–9617. [PubMed: 15210939]
31. Medintz IL, Clapp AR, Mattoussi H, Goldman ER, Fisher B, Mauro JM. Self-assembled nanoscale biosensors based on quantum dot FRET donors. Nat Mat 2003;2:630–638.
32. Medintz IL, Trammell SA, Mattoussi H, Mauro JM. Reversible modulation of quantum dot photoluminescence using a protein-bound photochromic fluorescence resonance energy transfer acceptor. J Am Chem Soc 2004;126:30–31. [PubMed: 14709044]
33. Sapsford KE, Medintz IL, Golden JP, Deschamps JR, Uyeda HT, Mattoussi H. Surface-immobilized self-assembled protein-based quantum dot nanoassemblies. Langmuir 2004;20:7720–7728. [PubMed: 15323524]
34. Medintz IL, Clapp AR, Melinger JS, Deschamps JR, Mattoussi H. A reagentless quantum dot sensing assembly based on förster resonance energy transfer. Adv Mater 2005;17:2450–2455.
35. Schnolzer M, Alewood P, Jones A, Alewood D, Kent SB. *In situ* neutralization in Boc-chemistry solid phase peptide synthesis. Rapid, high yield assembly of difficult sequences. Int J Pept Prot Res 1992;40:180–193.
36. Delehanty JB, Shaffer KM, Lin B. Transfected cell microarrays for the expression of membrane-displayed single-chain antibodies. Anal Chem 2004;76:7323–7328. [PubMed: 15595875]
37. Mosmann T. Rapid colorimetric assay for cellular growth and survival: application to proliferation and cytotoxicity assays. J Immunol Methods 1983;65:55–63. [PubMed: 6606682]
38. Hainfeld JF, Liu W, Halsey CMR, Freimuth P, Powell RD. Ni-NTA-Gold Clusters Target His-Tagged Proteins. J Struct Biol 1999;127:185–198. [PubMed: 10527908]
39. Goldman ER, Medintz IL, Hayhurst A, Anderson GP, Mauro JM, Iverson BL, Georgiou G, Mattoussi H. Self-assembled luminescent CdSe-ZnS quantum dot bioconjugates prepared using engineered poly-histidine terminated proteins. Anal Chim Acta 2005;534:63–67.
40. Ponnambalam S, Rabouille C, Luzio JP, Nilsson T, Warren G. The TGN38 glycoprotein contains two non-overlapping signals that mediate localization to the trans-Golgi network. J Cell Biol 1994;125:253–268. [PubMed: 8163544]
41. Thorstensen K, Romslo I. Uptake of iron from transferrin by isolated rat hepatocytes. A redox-mediated plasma membrane process? J Biol Chem 1988;263:8844–8850. [PubMed: 3379048]
42. Richard JP, Melikov K, Vives E, Ramos C, Verbeure B, Gait MJ, Chernomordik LV, Lebleu B. Cell-penetrating peptides. A reevaluation of the mechanism of cellular uptake. J Biol Chem 2003;278:585–590. [PubMed: 12411431]
43. Keminer O, Peters R. Permeability of single nuclear pores. Biophys J 1999;77:217–228. [PubMed: 10388751]
44. Midoux P, Monsigny M. Efficient gene transfer by histidylated polylysine/pDNA complexes. Bioconjugate Chem 1999;10:406–411.
45. Singh RS, Goncalves C, Sandrin P, Pichon C, Midoux P, Chaudhuri A. On the gene delivery efficacies of pH-sensitive cationic lipids via endosomal protonation: a chemical biology investigation. Chem Biol 2004;11:713–723. [PubMed: 15157882]
46. Hatefi A, Megeed Z, Ghandehari H. Recombinant polymer-protein fusion: a promising approach towards efficient and targeted gene delivery. J Gene Med. 2006In Press

47. Bentzen EL, Tomlinson ID, Mason J, Gresch P, Warnement MR, Wright D, Sanders-Bush E, Blakely R, Rosenthal SJ. Surface modification to reduce nonspecific binding of quantum dots in live cell assays. Bioconjugate Chem 2005;16:1488–1494.

48. Lovric J, Bazzi HS, Cuie Y, Fortin GR, Winnik FM, Maysinger D. Differences in subcellular distribution and toxicity of green and red emitting CdTe quantum dots. J Mol Med 2005;83:377–385. [PubMed: 15688234]

49. Shiohara A, Hoshino A, Hanaki K, Suzuki K, Yamamoto K. On the cyto-toxicity caused by quantum dots. Microbiol Immunol 2004;48:669–675. [PubMed: 15383704]

50. Saar K, Lindgren M, Hansen M, Eiriksdottir E, Jiang Y, Rosenthal-Aizman K, Sassian M, Langel U. Cell-penetrating peptides: a comparative membrane toxicity study. Anal Biochem 2005;345:55–65. [PubMed: 16137634]

51. Futaki S, Suzuki T, Ohashi W, Yagami T, Tanaka S, Ueda K, Sugiura Y. Arginine-rich peptides. An abundant source of membrane-permeable peptides having potential as carriers for intracellular protein delivery. J Biol Chem 2001;276:5836–40. [PubMed: 11084031]

52. Michalet X, Pinaud FF, Bentolila LA, Tsay JM, Doose S, Li JJ, Sundaresan G, Wu AM, Gambhir SS, Weiss S. Quantum dots for live cells, in vivo imaging, and diagnostics. Science 2005;307:538–544. [PubMed: 15681376]

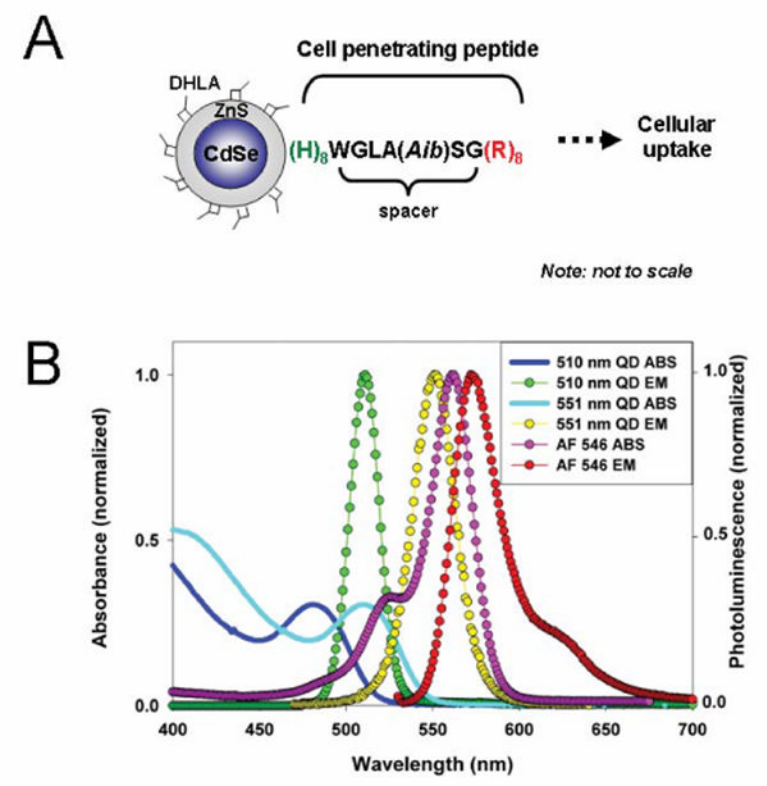

Figure 1. Schematic representation of a QD-peptide assembly and relevant absorbance/emission spectra for materials used in this study

(A) The peptide self-assembles onto the DHLA-capped CdSe/ZnS QD surface via $(His)_8$-Zn metal-affinity coordination. A short spacer separates the $(His)_8$ QD attachment domain from the HIV-1 Tat-derived $(Arg)_8$ cellular uptake sequence. Aib is α-amino isobutyric. (B) Absorbance of 510 nm and 551 nm QDs are represented by the solid black and cyan lines, respectively. The fluorescence spectra of the QDs and AlexaFluor 546 are also shown.

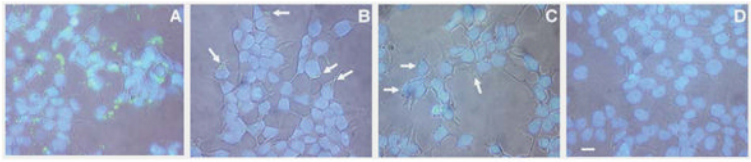

Figure 2. Dose-dependent cellular internalization of QD-CPP assemblies

HEK 293T/17 cells were incubated with 510-nm QD-CPP assemblies (QD:CPP ratio 1:50) at QD concentrations of: 250 nM (A), 60 nM (B), 15 nM (C) or with 250 nM QDs without CPP (D); cells were also stained with DAPI. Overlay of phase contrast, QD fluorescence (green), and DAPI fluorescence (blue) show the dose-dependent nature of the QD-CPP delivery. Images also show that QD staining is non-nuclear, punctate fluorescence located in the cytoplasm. Negligible cell-surface associated fluorescence was observed. Arrows indicate regions of QD-CPP internalization at lower concentrations. Scale bar is 10 μm.

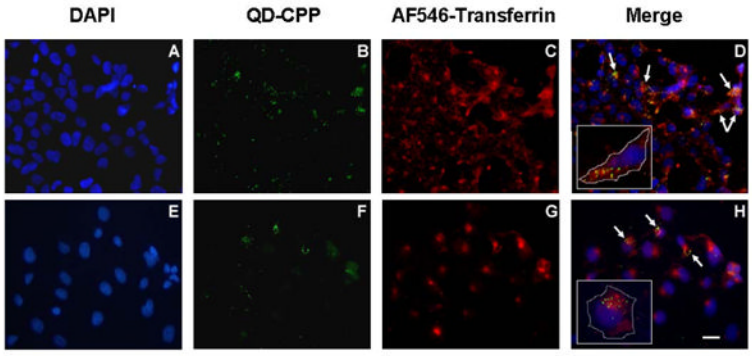

Figure 3. QD-CPP internalization and co-localization within endocytotic vesicles

HEK 293T/17 (A-D) and COS-1 (E-H) cells were co-incubated with 510 nm QD-CPP assemblies (QD:CPP ratio 1:25) and 40 μg/mL AlexaFluor 546-transferrin for one hour. Following washing and fixation, cells were imaged by epifluorescence. DAPI-stained nuclei are shown in panels A and E. QD fluorescence is shown in B and F and is largely perinuclear. Staining with AlexaFluor 546-transferrin, an endocytotic marker, is shown in C and G and merged images appear in D and H. The insets in D and H show representative single cells with the cell membrane marked for clarity. Arrows indicate areas of co-localization. Scale bar is 10 μm.

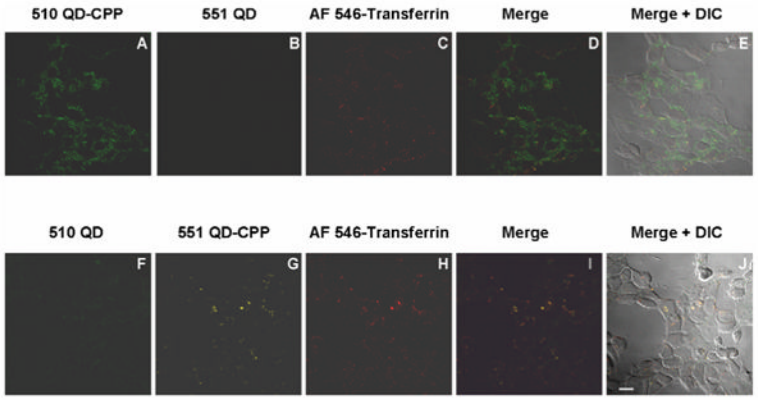

Figure 4. Selective cellular internalization of QD-CPP assemblies

HEK 293T/17 cells were incubated with mixtures of 510 nm QD-CPP (250 nM QD conc.) and unconjugated 551 nm QDs (60 nM) (in A-E) or to unconjugated 510 nm QDs (60 nM in QDs) and 551 nm QD-CPP (250 nM QD conc.) (in F-J). In both cases, cells were co-incubated with 40 μg/mL AF546-transferrin. The merged/DIC images show that assemblies are excluded from the nucleus. Scale bar is 10 μm.

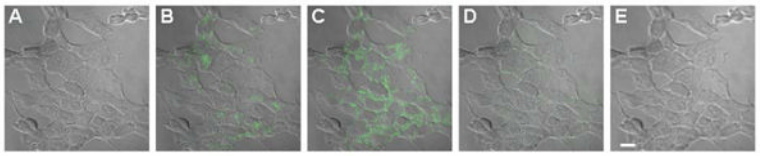

Figure 5. Laser scanning fluorescence images of cross-sectional slices along z-direction of internalized QD-CPP assemblies

HEK 293T/17 cells were incubated with a mixture of 510 nm QD-CPP conjugates (250 nM QD conc.) and unconjugated 551 nm QDs (60 nM in QDs). Sequential images (~0.4 μm sections with ~0.25 μm overlap between adjoining sections) were acquired along the z-axis. Panel (A) is below the cells while panel (E) is above the cells. Images show that QD fluorescence is located exclusively in the cytoplasm and is non-nuclear. After washing, no nonspecifically bound QDs remaining on the cell surface were observed. Scale bar is 10 μm.

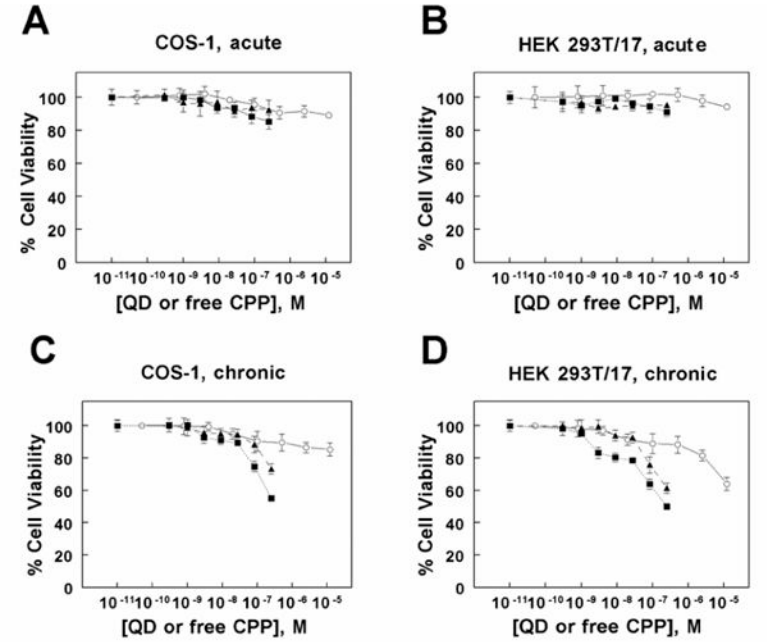

Figure 6. Differential cytotoxicity of QDs, CPP, or QD-CPP assemblies

The acute (short-term) and chronic (long-term) cytotoxicity of unconjugated QDs, free CPP, or QD-CPP assemblies (ratio QD:CPP = 1:25) was assessed using COS-1 and HEK 293T/17 cells. In the acute studies, COS-1 (panel A) and HEK 293T/17 (panel B) cells were incubated with the materials for one hour, washed, and subsequently cultured for 24 hours prior to viability assay. In the chronic studies, COS-1 (panel C) and HEK 293T/17 (panel D) cells were cultured for 24 hours in the presence of the materials prior to viability assay. Symbols correspond to: QD-CPP (■), unconjugated QDs (▲), and free CPP (○). For QD-CPP or unconjugated QDs, the concentrations designate those of the QDs. Each data point represents the mean ± SD of triplicate measurements.